Neutron excitations and interactions above the $N=80$ superdeformed closed shell: Superdeformation in ^{144}Eu

G. Hackman,* S. M. Mullins,† D. Haslip, S. Flibotte, J. A. Kuehner, and J. C. Waddington
Department of Physics and Astronomy, McMaster University, Hamilton, Ontario, Canada L8S 4M1

R. M. Clark
Lawrence-Berkeley National Laboratory, 1, Cyclotron Road, Berkeley, California 94550

S. Pilotte‡
Department of Physics, University of Ottawa, Ottawa, Ontario, Canada K1N 6N5
(Received 31 October 1996)

Three superdeformed bands have been observed in the nucleus ^{144}Eu with the GAMMASPHERE spectrometer in its early implementation phase. The reaction used was ^{122}Sn(^{27}Al,5n)^{144}Eu at a beam energy of 142 MeV. All three bands are identified as single-neutron excitations with respect to ^{143}Eu. One band is a confirmation of a previously suggested candidate. It is assigned as the yrast sequence based on the $\pi 6^1 \nu 7^1$ configuration, and is believed to undergo an interaction with the $\nu[514]9/2^-$ orbital. The other two bands are assigned as signature partners based on the $\pi 6^1 \nu \tilde{6}^1$ configuration, where $\tilde{6}$ corresponds to a mixed $[651]1/2^+/[642]5/2^+$ state. The partner that contains the $\alpha=-1/2$ signature component of the $\tilde{6}$ orbital is identified from a band crossing that occurs in related bands in ^{145}Gd and ^{146}Gd. Alignment plots suggest that the interaction strength becomes stronger as the mass number increases. [S0556-2813(97)03003-3]

PACS number(s): 27.60.+j, 21.10.Re, 23.20.Lv

I. INTRODUCTION

The investigation of chains of superdeformed nuclei at high spin allows the systematic study of active single-particle orbitals that are near the Fermi surface when the nuclear mean field is subjected to extreme distortion and rapid rotation. The first attempt to gain a systematic understanding of the single-particle structure along a chain was performed for the yrast superdeformed bands in the Gd isotopes [1]. More recently, valence-proton configurations have been established for the yrast superdeformed bands in the chain of $N=80$ isotones ^{142}Sm [2], ^{143}Eu [3,4], ^{144}Gd [5] and ^{145}Tb [6]. Attention has now focused on neutron excitations with respect to ^{143}Eu. A superdeformed band in ^{142}Eu [7] based on a hole in the $N=80$ closed SD shell has recently been found, whereas earlier evidence for superdeformation in ^{144}Eu comprised a ''ridge'' and a candidate band [8]. Here confirmation of this candidate as a *bona fide* superdeformed band is given, together with two new superdeformed bands that are assigned to ^{144}Eu. All three bands are interpreted as single-neutron excitations with respect to ^{143}Eu. Two of the bands show evidence for rotationally induced interactions caused by the crossing of neutron orbitals.

II. EXPERIMENT

The experiment was performed with an early implementation (EI) phase of the GAMMASPHERE multidetector γ-ray spectrometer located at the 88'' cyclotron building of the Lawrence Berkeley National Laboratory (LBNL). In this configuration the array consisted of 36 large volume hyperpure germanium (HPGe) detectors, each equipped with a bismuth germanate (BGO) Compton-suppression shield. A beam of ^{27}Al ions at an energy of 142 MeV was directed onto a target that consisted of a stack of two $\sim$500 μg/cm^2 foils enriched to $\sim$98% in ^{122}Sn. High-spin states in ^{144}Eu were populated in the 5n exit channel. The event trigger required that at least three suppressed HPGe signals were registered in coincidence after pileup rejection, such that the resolving time was 100 nsec, with each detector timed against the RF of the cyclotron. Typical ''singles'' HPGe rates were 10 KHz, with an event rate of 5–6 KHz. Gain and Doppler corrections were employed on line before digitization of the energy signals. The energies and times of the coincident γ rays were written onto magnetic cassettes for off-line analysis. Energy and relative efficiency calibrations of the HPGe detectors were obtained with ^{152}Eu and ^{133}Ba sources.

III. DATA ANALYIS AND RESULTS

The data were reduced off line to leave only the number and the energies of the detected γ rays for each event. These reduced data were stored in a compact format on magnetic cassette. Approximately 7.8×10^8 threefold, 2.8×10^8 fourfold, and 8.9×10^7 five to eightfold γ coincidences remained. These were unpacked into 2.9×10^9 threefold and 9.7×10^8 fourfold events. The threefold data were replayed into E_γ-

*Present address: Physics Divison, PHY-203 Argonne National Laboratories, 9700 South Cass Ave., Argonne, IL 60439.
†Present address: Department of Nuclear Physics, RSPhysSE, ANU, Canberra, ACT 0200, Australia.
‡Present address: Université Louis Pasteur, F-67037 Strasbourg Cedex 2, France.

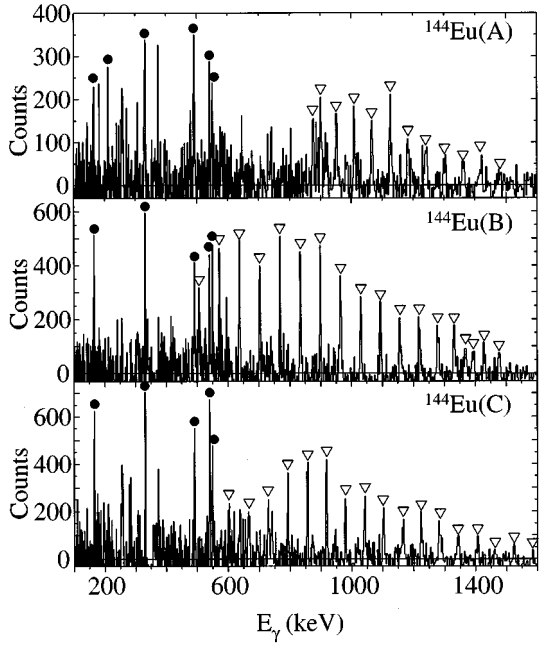

FIG. 1. Summed double-gated coincidence spectra generated with LEVIT8R that show the three superdeformed bands in ^{144}Eu. Each band member is indicated by a $\triangledown$, while non-SD transitions in ^{144}Eu are identified by a $\bullet$.

E_γ-E_γ cubes which were analyzed with the programs CUBEAID [9] and LEVIT8R [10]. This allowed fast and easy inspection of double-gated spectra.

Both the threefold and fourfold data were scanned for superdeformed bands of regular (but not necessarily constant) spacing with the code ANDBAND [11]. The starting energy was in the range $640 \leqslant E_0 \leqslant 711$ keV. Inspection of candidates put forward by the program suggested that four of them corresponded to superdeformed bands. One of these was the yrast band of ^{143}Eu [3,4], which will be referred to later as ^{143}Eu(A). Another proved to be a confirmation of the candidate that had been previously found with the 8π spectrometer [8]. The latter is now labeled as band A in ^{144}Eu [''^{144}Eu(A)'']. Two new sequences were also found, which are labeled as bands ^{144}Eu(B) and ^{144}Eu(C). Spectra generated with LEVIT8R for the three bands are shown in Fig. 1. Assignment to ^{144}Eu was based on coincidences with known transitions between the normal-deformed states in ^{144}Eu. This was helped by an extension of the level scheme with LEVIT8R. Double-gated and triple-gated spectra were generated for each SD band. These were compared in order to ascertain whether the appearance of transitions from normal-deformed states was real or random. The measured energies and intensities for each band are summarized in Table I.

The intensity pattern for each band was obtained from the double- and triple-gated data. In data of fold f, $f-1$ gates are set, and it is necessary to account for the effect of this gating procedure on the measured intensity pattern. A feeding pattern characteristic of superdeformed bands was assumed, namely an initial ''feeding ramp,'' a ''plateau'' followed by a sudden decay out. An iterative fit was peformed to this assumed feeding pattern, in which the detector efficiency was also included [12]. The results for the three bands are summarized in the Table I, where all intensities are compared to the maximum intensity of band C normalized to 1. It can be seen that within errors, the three bands are populated with the same maximum intensity relative to one another. The intensity with which ^{144}Eu(C) was populated relative to the total γ decay into the nucleus was determined from LEVIT8R. A figure of 0.17(4)% was obtained, while both ^{144}Eu(A) and ^{144}Eu(B) were populated at a maximum intensity of 0.14(4)%. Thus, under the present experimental conditions, the summed discrete-line superdeformed intensity in ^{144}Eu is estimated to be 0.45(7)%. This is approximately half the strength of the yrast bands in ^{143}Eu and ^{142}Eu.

TABLE I. Measured energies and intensities for the three superdeformed bands in ^{144}Eu.

^{144}Eu(A)		^{144}Eu(B)		^{144}Eu(C)	
E_γ (keV)	I_γ (%)	E_γ (keV)	I_γ (%)	E_γ (keV)	I_γ (%)
878.6(6)	0.39(8)	506.9(3)	0.36(8)	603.2(4)	0.61(14)
902.7(4)	0.63(8)	572.9(2)	0.65(12)	668.2(4)	0.61(9)
952.7(6)	0.57(12)	638.8(2)	0.76(13)	731.1(3)	0.63(9)
1011.7(5)	0.96(13)	638.8(2)	0.76(13)	794.2(3)	0.57(9)
1069.3(6)	0.88(14)	703.9(3)	0.61(9)	857.9(3)	1.06(10)
1128.0(6)	0.85(13)	769.5(2)	0.81(9)	919.1(1.2)	0.96(10)
1186.1(7)	0.64(14)	835.6(3)	0.93(10)	981.5(4)	0.99(10)
1244.9(6)	0.71(11)	900.7(3)	0.86(11)	1043.4(6)	1.16(13)
1302.2(8)	0.59(11)	966.4(3)	0.82(10)	1104.5(6)	0.68(10)
1363.3(9)	0.57(11)	1031.7(4)	0.85(11)	1165.3(6)	0.65(9)
1421.4(1.2)	0.46(13)	1095.6(5)	0.63(8)	1226.8(7)	0.47(8)
1478.6(2.1)	0.40(18)	1159.6(5)	0.63(9)	1284.3(6)	0.56(9)
		1221.6(5)	0.52(8)	1344.5(1.0)	0.43(8)
		1282.0(8)	0.50(7)	1403.2(1.0)	0.41(7)
		1334.6(6)	0.45(6)	1466.0(7)	0.34(6)
		1370.8(9)	0.28(6)	1528.0(1.3)	0.20(4)
		1396.5(1.1)	0.23(5)	1589.3(1.0)	0.16(5)
		1430.5(9)	0.19(5)		
		1467(1)	0.10(5)		

IV. DISCUSSION

A. Total Routhian surface calculations

Large gaps are known to occur in the Nilsson diagram at $Z=62$ and $N=80$ for a superdeformed shape which corresponds to $(\beta_2,\gamma)\simeq(0.5,0°)$. With respect to these gaps, the simplest valence configurations in ^{144}Eu are expected to be of the form $\pi 6^1 \nu X$, that is, single-neutron excitations with respect to the $N=80$ ''core'' nucleus, ^{143}Eu.

As a first step in the assignment of neutron configurations to the observed bands, we have performed total Routhian surface (TRS) calculations [13] for the four parity (π) and signature (α) combinations of the neutron orbital ''X.'' The proton component was kept fixed as $(\pi_\pi,\alpha_\pi)=(+,+\ 1/2)$ appropriate for the $\pi 6^1$ configuration. Hence the total quantum numbers of the system are given by $(\pi_{\rm tot},\alpha_{\rm tot})=(\pi_\nu,\ 1/2+\alpha_\nu)$.

All four configurations show a superdeformed minimum, as can be seen in Fig. 2. The calculations do not indicate that one particular configuration is markedly favored over the others, which is also the case for cranked Nilsson-Strutinksy calculations [14]. A moderately deformed triaxial minimum

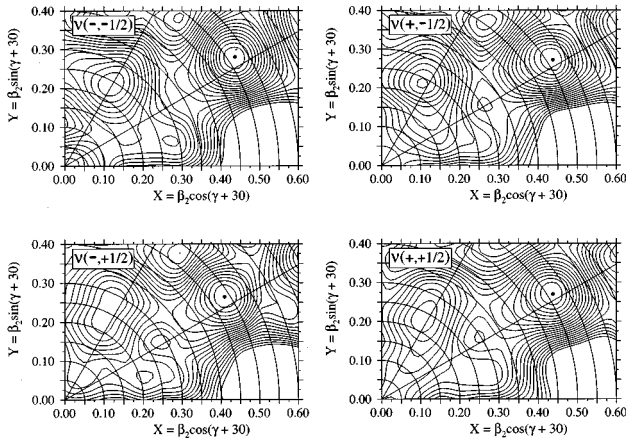

FIG. 2. Total Routhian surface calculations for ^{144}Eu for the four-parity signature (π,α) combinations for the odd neutron, as indicated in each panel. In each case the proton configuration is $(\pi,\alpha)=(+,+1/2)$, as appropriate for the occupancy of the $\pi 6^1$ intruder orbital.

is also common to each configuration, and collective structures believed to be based on this shape have been recently found in ^{144}Eu [15].

Since all four TRS minima have similar prolate deformations ($\beta_2=0.50\pm0.02$), one Routhian diagram can be used to guide the assignment of the neutron orbitals that correspond to the configurations represented by the TRS plots. Such a diagram is shown in Fig. 3; the proton Routhians are also shown for completeness.

At rotational frequencies greater than $\sim$0.5 MeV the Routhians suggest that the $\nu 7_1$ intruder orbital is likely to be

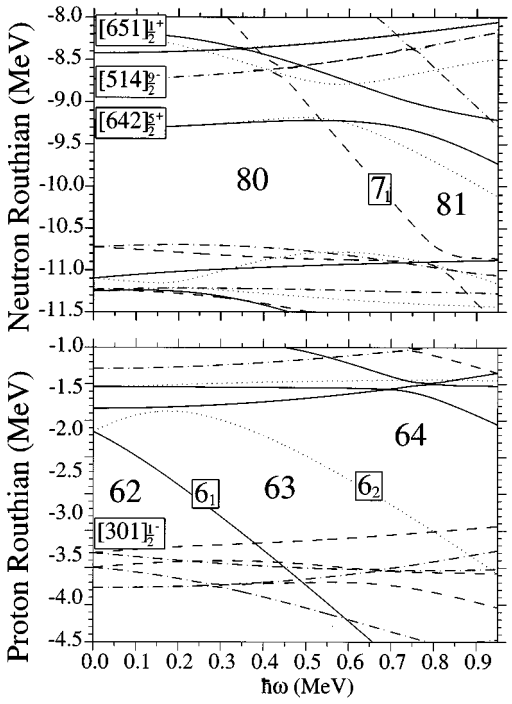

FIG. 3. Single-particle Routhians appropriate for ^{144}Eu calculated at $(\beta_2,\beta_4,\gamma)=(0.52,0.05,3°)$. Important orbitals and particle numbers have been labeled, as fully explained in the text.

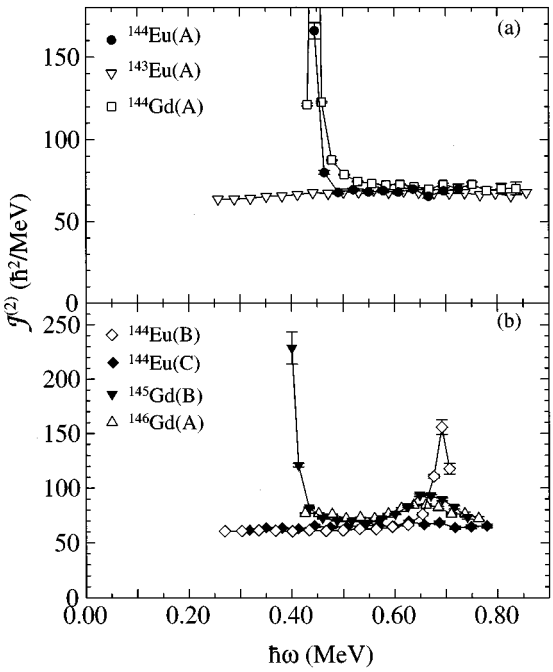

FIG. 4. $\mathcal{J}^{(2)}$ dynamic moments of inertia for the three superdeformed bands in ^{144}Eu compared with those for some superdeformed bands in nearby nuclei. [Note, in (a) the $\mathcal{J}^{(2)}$ for ^{144}Gd(A) goes off scale.]

occupied in the yrast configuration. This corresponds to the neutron $(-,-1/2)$ configuration. Hence the high-$N_{\rm osc}$ (where $N_{\rm osc}$ is the major oscillator quantum number) configuration of the yrast superdeformed band in ^{144}Eu is expected to be $\pi 6^1 \nu 7^1$. The candidate band that was previously found with the 8π spectrometer was tentatively identified with this configuration. Since the $(\pi_{\rm tot},\alpha_{\rm tot})$ quantum numbers of this configuration are $(-,0)$, the corresponding band has negative parity and even spins.

Over the same frequency range, the lowest lying excited band is predicted to be based on a positive-parity Routhian of negative signature. We shall label this state and its signature partner as $\tilde{6}_{\alpha=\pm1/2}$, since they arise from the crossing of routhians that originate from the $[651]1/2^+$ and $[642]5/2^+$ Nilsson levels. Indeed, the crossing of the negative-signature Routhians is believed to be responsible for ''humps'' that are observed in the dynamic moments of the excited and yrast superdeformed bands in ^{145}Gd [''^{145}Gd(B)''] [16] and ^{146}Gd [''^{146}Gd(A)''] [17,18], respectively. Hence a similar feature would be expected in the first excited band in ^{144}Eu.

B. Dynamic moments of inertia: Configuration assignments

The dynamic moments of inertia have been extracted for each band from the energy differences of successive transitions. They are shown in Figs. 4(a) and (b), together with those from other relevant superdeformed bands. In the $A=140-150$ region, the sensitivity of the $\mathcal{J}^{(2)}$ moment of inertia to the high-$N_{\rm osc}$ occupancy can be extremely useful when it comes to making configuration assignments. In the present case, the configuration assignments have to be con-

sistent with the dramatic rises that occur in ^{144}Eu(A) and ^{144}Eu(B) at $\hbar\omega \simeq 0.45$ MeV and 0.69 MeV, respectively.

1. ^{144}Eu(A)

It was previously suggested that the candidate band (now confirmed here as band A) found in ^{144}Eu was the yrast sequence based on the $\pi 6^1 \nu 7^1$ configuration. The lowest transition energy of the candidate was identified as 894 keV, which may be compared to 483 keV in the yrast band in ^{143}Eu. This large difference was hard to understand, since a band crossing or unpaired-to-paired phase transition which would force a rapid decay out of the band, was not expected for this configuration. The suspicion was that the band could not be followed to lower transition energies due to its weakness. In fact, the shortness of the band was confirmed in the present high-fold data, where it can now be seen that the $\mathcal{J}^{(2)}$ of ^{144}Eu(A) undergoes a dramatic rise at $\hbar\omega \simeq 0.45$ MeV. This clearly suggests that the band is undergoing a structural change, at which point it disappears. It is believed (see below) that the change in structure arises from the crossing of the $\nu 7_1$ intruder and the negative-signature Routhian that originates from the [514]9/2$^-$ orbital. Hence, the assignment of ^{144}Eu(A) to the yrast $\pi 6^1 \nu 7^1$ configuration is consistent with the present data.

For completeness, it should be noted that the behavior of the $\mathcal{J}^{(2)}$ of ^{144}Eu(A) is reminiscent of that seen in ^{144}Gd(A) and ^{145}Gd(B) (see Fig. 4). In these cases the rise is attributed to a quasiproton crossing due to the alignment of the first pair of $N_{\rm osc}=6$ proton intruders. This could only happen in ^{144}Eu(A) if the band were based on a proton excitation of the form $\pi 6^2 \otimes X^{-1}$. Such a configuration could be considered as a proton hole in ^{145}Gd(A). Inspection of the proton Routhian diagram suggests that the vacated orbital ''X'' would most probably correspond to the negative-signature Routhian that originates from the [301]1/2$^-$ Nilsson level. A hole in this orbital would be expected to give rise to a band with identical transition energies to ^{145}Gd(A), since the signature (α) has the same sign and value as the aligned spin (i). This is not the case, and, moreover, there is no evidence for the quasiproton crossing in ^{145}Gd(A) which is clearly observed in ^{145}Gd(B) [16]. This may be due to the weaker proton pairing in ^{145}Gd(A) that arises from an increase in deformation caused by the occupation of the $\nu 7_1$ intruder orbital [16]. Since there is evidence that SD bands based on the same high-$N_{\rm osc}$ intruder configuration have the same quadrupole deformation [19], it seems unlikely that the quasiproton crossing would appear in ^{144}Eu(A) when it does not occur in ^{145}Gd(A).

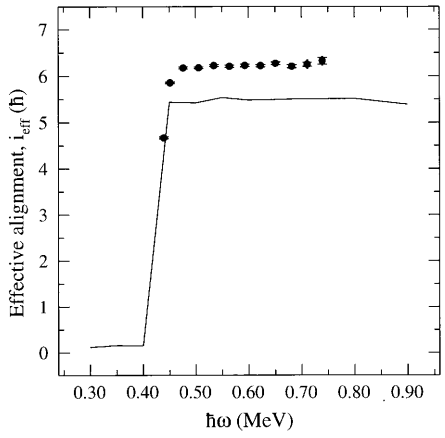

FIG. 5. Effective alignment for ^{144}Eu(A) relative to ^{143}Eu(A). The line shows the $i_{\rm eff}$ for the $\nu 7_1$ intruder orbital predicted by the Hartree-Fock calculations. The drop at low frequency occurs when the $\nu 7_1$ intruder crosses the [514]9/2$^-$ orbital.

2. ^{144}Eu(B)

The $\mathcal{J}^{(2)}$ of ^{144}Eu(B) shows a dramatic rise close to the frequency where the ''humps'' are observed in ^{145}Gd(B) and ^{146}Gd(A), as shown in Fig. 4(b). Hence, it seems reasonable to identify ^{144}Eu(B) with the excited neutron configuration, $\pi 6^1 \nu \tilde{6}_{\alpha=-1/2}$. A comparison of interaction strength of the orbital crossing that causes the perturbations in these bands will be made in a later section.

3. ^{144}Eu(C)

The most likely assignment for ^{144}Eu(C) is the (+,1) signature partner to ^{144}Eu(B), namely the $\pi 6^1 \nu \tilde{6}_{\alpha=+1/2}$ configuration. The cranking models show that an interaction is also expected in this band, but the $\alpha=+1/2$ orbitals cross at frequency beyond that observed experimentally.

C. Effective alignment of the $\nu 7_1$ intruder orbital

The interpretation of the intrinsic structure of superdeformed bands is, in general, based on the behavior of the $\mathcal{J}^{(2)}$ as a function of rotational frequency. This approach is a consequence of the lack of knowledge of the spins (and pari-

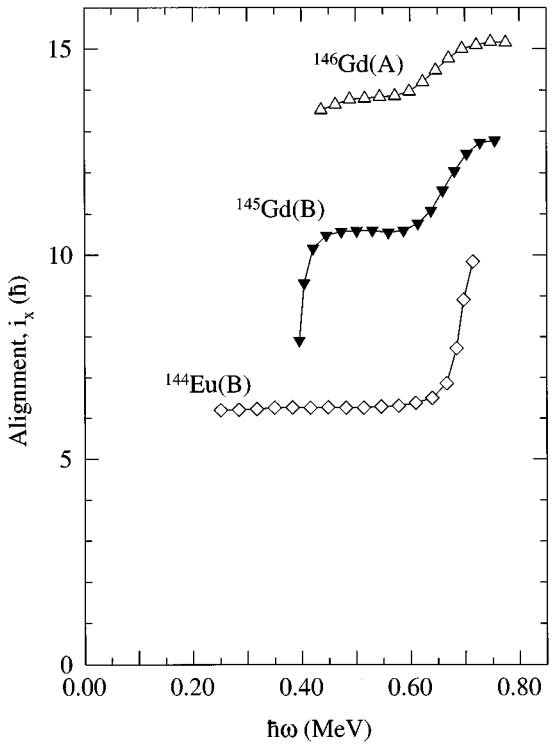

FIG. 6. Aligned spins for ^{144}Eu(B), ^{145}Gd(B), and ^{146}Gd(A). The Harris parameters that were used are listed in Table II.

TABLE II. Spin values and Harris parameters used to extract the gain in aligned spin through the $\alpha=-1/2[651]1/2^+/[642]5/2^+$ crossing in ^{144}Eu(B), ^{145}Gd(B), and ^{146}Gd(A). The aligned spins are plotted in Fig. 6.

Nucleus (band)	Config^n	E_γ (keV)	$I_i \rightarrow I_f(\hbar)$	$\langle K\rangle(\hbar)$	$\mathcal{J}_0(\hbar^2\mathrm{MeV}^{-1})$, $\mathcal{J}_1(\hbar^4\mathrm{MeV}^{-3})$	$\Delta i(\hbar)$
^{144}Eu(B)	$\pi 6^1 \nu \tilde{6}_{\alpha=-1/2}$	507	22	3	60.0, 2.0	$\geqslant 4.4$
^{145}Gd(B)	$\pi 6^2 \nu \tilde{6}_{\alpha=-1/2}$	793	35.5	4.5	68.0, 2.0	2.2
^{146}Gd(A)	$\pi 6^1 \nu \tilde{6} \otimes 7^1$	826	43	5	70.0, 2.0	1.3

ties) of the vast majority of SD bands. Hence, the quantization of angular momentum, and the fact that even-A (odd-A) systems have integer (half-integer) spins are of no use when only the $\mathcal{J}^{(2)}$ is considered. These facts can be exploited when an analysis in terms of effective alignments [20] is employed. In this approach, the relative change in spin at a particular rotational frequency can be inferred from nucleus ''A'' to nucleus ''$A+1$'' as a particle is added. This difference in spin at a particular rotational frequency is called the ''effective alignment'' (i_{eff}), which can be compared with a theoretical prediction for a particle placed in a specific orbital. It is assumed that changes in other quantities, such as pairing and deformation, due to the addition of the particle are small compared to the effect of the orbital spin. The aim of an analysis based on effective alignments is therefore to mutually assign spins and configurations in a consistent way over a range of nuclei. This was first attempted for the yrast superdeformed bands in the chain of gadolinium nuclei from ^{146}Gd to ^{150}Gd [1]. Effective alignments were derived for the various neutron orbitals that are filled from as the neutron number increased from $N=82$ to 86. Since the $\nu 7_1$ intruder orbital is occupied in all of these bands, it was not possible to extract its effective alignment.

The subsequent discovery of SD bands in ^{144}Gd ($N=80$) [5] and ^{145}Gd ($N=81$) [16] has meant, in principle, the alignment could be obtained from the latter when compared with the former. The strong perturbation of the level spacing caused by the $N=6$ quasiproton crossing in ^{144}Gd, however, hampers the analysis. A more reliable way of obtaining the i_{eff} of the $\nu 7_1$ orbital is to compare the $\pi 6^1 \nu 7^1$ yrast configuration in ^{144}Eu with the yrast band in ^{143}Eu. In the analysis it has been assumed that, consistent with the results of [4] and the signature of $+1/2$, the 484 keV transition in ^{143}Eu(A) decays to a $37/2\hbar$ state. The yrast $\pi 6^1 \nu 7^1$ configuration in ^{144}Eu will have even spin, since the signature is zero. The effective alignment so derived is shown in Fig. 5, where it is compared with a theoretical prediction for the $\nu 7_1$ orbital taken from unpaired Hartree-Fock calculations [21]. It is from this comparison that the 879 keV transition has been assigned to decay from a $38\hbar$ state, since this gives the best agreement with theory. The effective alignment is constant apart from sudden decrease at the lowest frequency, which suggests that the orbital occupied by the 81st neutron in ^{144}Eu(A) has a constant alignment over almost the entire observed frequency range. The constancy is well reproduced by the Hartree-Fock calculations, as is the drop at lower frequencies, where the calculations converge to a minimum that corresponds to the occupancy of the $\nu[514]\ 9/2^-$ orbital, which has a negligible aligned spin.

D. Characteristics of the $\alpha=-1/2[651]1/2^+/[642]5/2^+$ crossing

Evidence has now been seen in three[1] SD bands for the crossing of the $\alpha=-1/2$ neutron orbitals that originate from the $[651]1/2^+$ and $[642]5/2^+$ Nilsson levels. The characteristics of the two orbitals [see Fig. 3(a)] means that the crossing can only occur if the former lies higher in energy than the latter at zero rotation. Woods-Saxon mean-field calculations [13] predict that these two orbitals cross at $\beta_2 \simeq 0.6$. Since the Nilsson states originate from the $l=6$ $i_{11/2}$ and $i_{13/2}$ spherical subshells, respectively, the crossing provides a sensitive test of the mean-field parameters.

1. Gain in aligned spin through the crossing.

Though the spins of the three bands in question are not known, it is possible to extract the gain in aligned spin that results from the crossing. The configuration assignments to the three bands can be used to limit the relative spins between the three bands, and also to choose the K quantum number, which was taken as the sum of the K values of the valence particles. These values are listed in Table II, together with the Harris parameters used to subtract off the collective component of the spin. It should be noted that the gain in aligned spin is insensitive to changes in either K or the assigned spins, since the former is small compared to the latter.

Inspection of the aligned spins (see Fig. 6) and $\mathcal{J}^{(2)}$ plots clearly suggests that the interaction strength is weakest in ^{144}Eu(B), due to the more abrupt upbend at the crossing. The plots indicate that the interaction strength increases from ^{144}Eu(B) to ^{145}Gd(B) to ^{146}Gd(A). This trend probably reflects an increase in deformation, since, as shown in Table II, the number of occupied high-j intruder orbitals increases by one from ^{144}Eu(B) ($\pi 6^1$) to ^{145}Gd(B) ($\pi 6^2$) to ^{146}Gd(A) ($\pi 6^2 \nu 7^1$). Only in the case of ^{146}Gd(A) has the deformation been inferred from Doppler shift lifetime measurements [17], but it is hoped that the relative differences in deformation between these bands can be measured in the near future with a large detector array.

2. Quantification of the interaction strength

It should be possible to quantify the interaction strengths by inserting the gain in aligned spin (Δi), the maximum ($\mathcal{J}^{(2)}_{\mathrm{max}}$) and unperturbed ($\mathcal{J}^{(2)}_0$) values of the $\mathcal{J}^{(2)}$ into the equation

[1]There is now probably a fourth case in the $N=81$ nucleus ^{143}Sm [22].

TABLE III. Estimated interaction frequencies and strengths for the $\alpha=-1/2[651]1/2^+/[642]5/2^+$ crossing in ^{144}Eu(B), ^{145}Gd(B), and ^{146}Gd(A).

Nucleus (band)	$\Delta i(\hbar)$	$\mathcal{J}_0^{(2)}$ ($\hbar^2$ MeV^{-1})	$\mathcal{J}_{\max}^{(2)}$ ($\hbar^2$ MeV^{-1})	$\hbar\omega_{\rm int}$ (MeV)	$V_{\rm int}$ (keV)
^{144}Eu(B)	$\geqslant$4.4	62	155	0.69	$\geqslant$130
^{145}Gd(B)	2.2	69	93	0.67	67
^{146}Gd(A)	1.3	72	85	0.64	38

$$V_{\rm int}=\frac{1}{4}\Delta i^2\frac{\mathcal{J}_{\max}^{(2)}}{\mathcal{J}_0^{(2)}(\mathcal{J}_{\max}^{(2)}-\mathcal{J}_0^{(2)})} \quad (1)$$

which is derived under the assumption that the crossing bands interact a fixed spin [23], rather than at a fixed rotational frequency [24–26]. The quantities Δi, $\mathcal{J}_{\max}^{(2)}$ and $\mathcal{J}_0^{(2)}$ are listed in Table III for the three bands, together with the interaction strengths calculated from Eq. (1).

It can be seen from Table III that the interaction strengths derived from Eq. (1) display the opposite trend than that inferred from inspection of the aligned spin. That is, the interaction strength increases from ^{144}Eu(B) to ^{145}Gd(B) to ^{146}Gd(A). Indeed, the interaction strength for ^{144}Eu(B) is about a factor of 2 larger than in ^{145}Gd(B), and over a factor of 3 larger than in ^{146}Gd(A). This disagreement probably reflects that the assumptions made in the derivation of Eq. (1) are not justified, particularly those concerning the constancy and equality of $\mathcal{J}_0^{(2)}$ for the two interacting bands. It is interesting to note, however, that the calculations of [23] predict that the interaction strength increases as the deformation decreases, in agreement with the results obtained with Eq. (1).

V. CONCLUSIONS

Three superdeformed bands have been observed in ^{144}Eu. One band is a confirmation of the candidate found in a previous experiment. It is identified as the yrast sequence which is based on a $\pi 6^1\nu 7^1$ high-$N_{\rm osc}$ intruder configuration. Relative to the $N=80$ closed SD shell, it is simply a single-neutron excitation into the $\nu 7_1$ orbital. The effective alignment of this band has been extracted relative to ^{143}Eu. Both the constancy and sudden decrease at low rotational frequencies of the effective alignment are well reproduced by a Hartree-Fock calculation for the $\nu 7_1$ orbital.

The other two bands have been interpreted as signature partners based on the $\pi 6^1\nu\tilde{6}^1$ excited configuration, where $\tilde{6}$ correponds to a mixture of the $[651]1/2^+$ and $[642]5/2^+$ Nilsson states. One of the bands undergoes a crossing at $\hbar\omega\simeq 0.69$ MeV, similar to that seen in the yrast SD band of ^{146}Gd and in the first excited SD band of ^{145}Gd. It is therefore identified as the $\alpha=-1/2$ signature component. Alignment plots for the three bands suggest that the interaction strength of the crossing is weakest in ^{144}Eu, whereas the opposite is true if the interaction strength is extracted with a standard band-mixing formula.

ACKNOWLEDGMENTS

This work was supported by the Natural Sciences and Engineering Research Council of Canada and AECL Research. We thank the crew at the 88'' cyclotron for supplying the beam and P. Dmytrenko for making the target. The CSM and TRS codes were kindly made available to us by Dr. R. A. Wyss. We also thank Dr. J. Dobaczewski and Dr. J. Dudek for the use of the Hartree-Fock codes.

[1] B. Haas, V. P. Janzen, D. Ward, H. R. Andrews, D. C. Radford, D. Prévost, J. Kuehner, A. Omar, J. C. Waddington, T. E. Drake, A. Galindo-Uribarri, G. Zwartz, S. Flibotte, P. Taras, and I. Ragnarsson, Nucl. Phys. **A561**, 251 (1993).

[2] G. Hackman, S. M. Mullins, J. A. Kuehner, D. Prévost, J. C. Waddington, A. Galindo-Uribarri, V. P. Janzen, D. C. Radford, N. Schmeing, and D. Ward, Phys. Rev. C **47**, 433 (1993).

[3] S. M. Mullins, R. A. Wyss, P. Fallon, T. Byrski, D. Curien, S. A. Forbes, Y -J. He, M. S. Metcalfe, P. J. Nolan, E. S. Paul, R. J. Poynter, P. H. Regan, and R. Wadsworth, Phys. Rev. Lett. **66**, 1677 (1991).

[4] A. Ataç, M. Piiparinen, B. Herskind, J. Nyberg, G. Sletten, G. de Angelis, S. Forbes, N. Gjøup, G. Hagemann, F. Ingebretsen, H. Jensen, D. Jerrestam, H. Kusakari, R. M. Lieder, G. V. Marti, S. Mullins, D. Santonocito, H. Schnare, K. Strähle, M. Sugawara, P. O. Tjøm, A. Virtanen, and R. Wadsworth, Phys. Rev. Lett. **70**, 1069 (1993).

[5] S. Lunardi, D. Bazzacco, C. Rossi-Alvarez, P. Pavan, G. de Angelis, D. De Acuna, M. De poli, G. Maron, J. Rico, O. Stuch, D. Weil, S. Utzelmann, P. Hoernes, W. Satula, and R. Wyss, Phys. Rev. Lett. **72**, 1427 (1994).

[6] S. M. Mullins, N. C. Schmeing, S. Flibotte, G. Hackman, J. L. Rodriguez, J. C. Waddington, L. Yao, H. R. Andrews, A. Galindo-Uribarri, V. P. Janzen, D. C. Radford, D. Ward, J. DeGraaf, T. E. Drake, S. Pilotte, and E. S. Paul, Phys. Rev. C **50**, R2261 (1994).

[7] S. M. Mullins, S. Flibotte, G. Hackman, J. L. Rodriguez, J. C. Waddington, A. V. Afanasjev, I. Ragnarsson, H. R. Andrews, A. Galindo-Uribarri, V. P. Janzen, D. C. Radford, D. Ward, M. Cromaz, J. DeGraaf, T. E. Drake, and S. Pilotte, Phys. Rev. C **52**, 99 (1995).

[8] S. M. Mullins, G. Hackman, A. Galindo-Uribarri, D. C. Radford, J. C. Waddington, and D. Ward, Z. Phys. A **346**, 327 (1993).

[9] J. A. Kuehner, J. C. Waddington, and D. Prévost, *Proceedings of the Workshop on Large Gamma-Ray Detector Arrays*, Chalk River Laboratories, 1992 (AECL Report 10613), Vol. 2, p. 413.

[10] D. C. Radford, Nucl. Instrum. Methods Phys. Res. A **361**, 297 (1994).
[11] D. S. Haslip, G. Hackman, and J. C. Waddington, Nucl. Instrum. Methods Phys. Res. A **345**, 534 (1994).
[12] G. Hackman, Ph.D. thesis, McMaster University, Hamilton, Ontario, Canada, 1996.
[13] W. Nazarewicz, R. Wyss, and A. Johnson, Nucl. Phys. **A503**, 285 (1989).
[14] A. V. Afanasjev and I. Ragnarsson, private communication.
[15] M. Piiparinen, A. Ataç, S. J. Freeman, R. Julin, S. Juutinen, A. Lampinen, T. Lönroth, D. Müller, J. Nyberg, G. Sletten, P. Tikkanen, S. Törmänen, A. Virtanen, C. T. Zhang, and R. Wyss, Phys. Rev. C **52**, R1 (1995).
[16] T. Rzaça-Urban, R. M. Lieder, S. Utzelmann, W. Gast, A. Georgiev, H. M. Jäger, D. Bazzacco, S. Lunardi, R. Menegazzo, G. Rossi-Alverez, G. de Angelis, D. R. Napoli, G. Vedovato, and R. Wyss, Phys. Lett. B **356**, 456 (1995).
[17] G. Hebbinghaus, K. Strähle, T. Rzaça-Urban, D. Balabanski, W. Gast, R. M. Lieder, H. Schnare, and W. Urban, Phys. Lett. B **240**, 311 (1990).
[18] C. Schumacher, O. Stuch, T. Rzaça-Urban, P. von Brentano, A. Dewald, A. Georgiev, R. Lieder, F. Linden, J. Lisle, T. Theuerkauf, W. Urban, S. Utzelmann, and D. Weißhaar, Phys. Rev. C **52**, 1302 (1995).
[19] H. Savajols, A. Korichi, D. Ward, D. Appelbe, G. C. Ball, C. Beausang, F. A. Beck, T. Byrski, D. Curien, P. Dagnall, G. de France, D. Disdier, G. Dûchene, S. Erturk, C. Finck, S. Flibotte, B. Gall, A. Galindo-Uribarri, B. Haas, G. Hackman, V. P. Janzen, B. Kharraja, J. C. Lisle, J. C. Merdinger, S. M. Mullins, S. Pilotte, D. Prévost, D. C. Radford, V. Rauch, C. Rigollet, D. Smalley, M. B. Smith, O. Stezowski, J. Styczen, Ch. Theisen, P. J. Twin, J. P. Vivien, J. C. Waddington, K. Zuber, and I. Ragnarsson, Phys. Rev. Lett. **76**, 4480 (1996).
[20] Ingemar Ragnarsson, Nucl. Phys. **A557**, 167c (1993).
[21] J. Dobaczewski and J. Dudek, submitted to Comput. Phys. Commun.
[22] H.-Q. Jin, C. Baktash, M. J. Brinkman, D. Rudolph, C.-H. Yu, R. M. Clark, M. Devlin, P. Fallon, D. R. LaFosse, I.-Y. Lee, F. Lerma, A. O. Macchiavelli, and D. G. Sarantites, *Proceedings of the Conference on Nuclear Structure at the Limits* (Report ANL/PHY-96/1, 1996).
[23] S. Åberg, Nucl. Phys. **A520**, 35c (1990).
[24] V. P. Janzen, H. R. Andrews, B. Haas, D. C. Radford, D. Ward, A. Omar, D. Prévost, M. Sawicki, P. Unrau, J. C. Waddington, T. E. Drake, A. Galindo-Uribarri, and R. Wyss, Phys. Rev. Lett. **70**, 1065 (1993).
[25] Ragnar Bengtsson and Sven Åberg, Phys. Rev. Lett. **72**, 3288 (1994).
[26] V. P. Janzen, R. Wyss, and N. C. Schmeing, Phys. Rev. Lett. **72**, 3289 (1994).